Recent advances in the development of ultrafast electronic circular dichroism for probing the conformational dynamics of biomolecules in solution

Pascale Changenet, François Hache

Eur. Phys. J. Special Topics (2022)

https://doi.org/ 10.1140/xxxxx (will be inserted by the publisher)

Recent advances in the development of ultrafast electronic circular dichroism for probing the conformational dynamics of biomolecules in solution

Pascale Changenet* and François Hache

Laboratoire d'Optique et Biosciences, CNRS, INSERM, Ecole Polytechnique, Institut Polytechnique de Paris, 91128 Palaiseau, France

Abstract. Conformational dynamics of biomolecules, which can span very large time scales ranging from seconds down to femtoseconds, play a key role in their function. In this regard, the combination of the high temporal resolution of ultrafast pump-probe spectroscopy and the structural sensitivity of electronic circular dichroism (CD) spectroscopy provides an extremely promising tool to follow these dynamics with a "virtually" unlimited temporal resolution. However, although CD spectroscopy is a widely used tool in structural biology to determine the secondary structure of biomolecules in solution, transposition of these measurements to the time domain (TRCD), on the sub-picosecond time scale, remains very challenging due to their weak signals, prone to pump-induced polarization artifacts. Recent advances in laser technologies and non-linear optics however offer new perspectives for the development of femtosecond TRCD set-ups. In this review, we present recent developments in ultrafast TRCD spectroscopy. We discuss the advantages and drawbacks of the few existing functional experimental set-ups for their use to access the conformational dynamics of biomolecules at ultrashort time scales.

1. Introduction

Conformational dynamics of biomolecules are intimately related to their function. Capturing these dynamics which can occur on a wide range of time scales spanning from femtoseconds to seconds remains a major issue of modern biophysics. In this regard, ultrafast "pump-probe" spectroscopy provides an incisive tool to obtain fundamental information about their dynamical behavior over a broad spectral range, with "virtually" unlimited temporal resolution. The basic principle of pump-probe spectroscopy relies on the measurement of the third order nonlinear optical response of a medium following the interaction with a sequence of ultrashort optical pulses. In its simplest configuration, namely transient absorption, a first strong laser "pump" pulse is used as the perturbation to trigger a photoinduced reaction and a second weaker "probe" pulse is used to monitor the pump-induced changes in the studied medium. While femtosecond UV-visible transient absorption spectroscopy is nowadays a commonly used tool in laboratories for probing the excited-state dynamics of photoactivatable molecules, monitoring their conformational changes in the course of their deactivation is still an experimental challenge, which requires to combine high time resolution with structural sensitivity in a pump-probe set-up. In this regard, the development of commercial ultrafast laser sources has facilitated the implementation of increasingly sophisticated pump-probe setups, allowing to access the structural dynamics of complex molecular assemblies with a femtosecond time resolution (for recent reviews see [1-4]). Notably, femtosecond infrared (IR) transient spectroscopy and 2-dimensional IR spectroscopy have now become well-established tools for probing the conformational changes of photoactivable biomolecules [5-8], but with the major drawback stemming from the strong absorption of aqueous biological solvents in the frequency domain around ca. 1600 cm^{-1} and ca. 3700 cm^{-1} and their difficulty to distinguish the vibrational modes in action requiring site-specific labeling.[9] In the meantime, femtosecond stimulated Raman scattering spectroscopy has gained a specific attention, as a label-free probe, providing vibrational structural information about the excited state of photoactivable protein chromophores [2,10-12]. More recently, the combination of X-ray free electron lasers (XFEL) and femtosecond UV-visible laser pump, namely serial femtosecond crystallography (SFX), has been also used to track the conformational changes of several photoactive proteins at the "atomic scale" [13]. As an alternative to SFX, chiroptical spectroscopy, *i.e.* chirality-sensitive spectroscopy, provides a versatile tool to study the structural changes of biomolecules in condensed phase, under near-physiological conditions. More specifically, circular dichroism (CD), which is the differential absorbance between left- and right-handed circularly polarized light, is a very popular technique for analyzing the secondary structure of biomolecules at equilibrium in solution, with the advantage that their CD spectra in the

spectral region between 200 and 300 nm can be theoretically or phenomenologically related to their conformation [14,15]. In this context, the combination of CD and pump-probe spectroscopy provides a promising tool for investigating the conformational change of chiral compounds over a large time domain, with a table-top configuration. However, despite the conceptual simplicity of the principle of steady-state measurements, transposition of CD spectroscopy to the time domain (TRCD), especially on the sub-picosecond time scale remains scarce due to their weak signals, *i.e.* two to five orders of magnitude weaker than those of conventional transient absorption, that are prone to pump-induced artifacts [16]. Recent improvements in laser technologies and in the polarization control of ultrashort laser pulses down to the deep UV spectral domain however provides renewed opportunities for the development of new TRCD detection strategies to access the conformational changes of chiral compounds with an increased sensitivity [17-20]. In this review, we give an overview of the recent key technological advances in the development of ultrafast TRCD spectroscopy. We discuss the main advantages and drawbacks of the existing functional experimental set-ups for accessing the conformational dynamics of (bio)molecules. We then address the open challenges and directions for the current developments of femtosecond TRCD set-ups.

2. Chirality in (bio)molecules

The term chirality is derived from the Greek word *keir* which means hand. It describes objects that are not superimposable to their image in a mirror, at any scale. In chemistry, chiral molecules can exist in two forms called enantiomers. In achiral environments, enantiomers have identical chemical properties, while in chiral environments, they interact differently and can therefore be differentiated. Molecular chirality is a ubiquitous property in nature. In particular, proteins and nucleic acids are chiral molecular assemblies made of elementary building blocks themselves chiral. In living organisms, these building blocks display mainly in a single enantiomeric form, the left one for amino acids and the right one for sugars. Although the origin of this homochirality remains an open question about the origin of life, it is well established that it plays a key role in the fundamental processes of molecular recognition in biology.

From the physical point of view, chiral molecules exhibit an optical activity. They absorb differently left- and right-circularly polarized light, an absorbance property called circular dichroism (CD), which is defined as:

$$CD = \Delta\varepsilon \cdot l \cdot c = (\varepsilon_L - \varepsilon_R) \cdot l \cdot c \qquad (1)$$

with $\Delta\varepsilon = \varepsilon_L - \varepsilon_R$, the difference in the molar extinction coefficients between left- and right-circularly polarized light respectively. l is the optical path and c, the sample concentration. Chiral compounds have also the ability to rotate the plane of polarization of linearly polarized light, a dispersive property called optical rotatory dispersion (ORD) which is defined as:

$$ORD = 2\pi \cdot (n_R - n_d) \cdot l/\lambda \qquad (2)$$

with λ, the wavelength. The optical activity of chiral compounds is related to their electronic structure. For instance, the intrinsic chirality of the asymmetric atoms, such as the carbon of amino acids and sugars can be described by the coupling of their electric dipole transition moment and their magnetic transition moment between the ground and excited states. In complex molecular assemblies, such as in proteins or DNA, chirality arises from the coupling of their electric dipole transition moments located on the different chromophores and therefore strongly depends on their spatial arrangement. In proteins, α-helices and β-sheets display characteristic CD spectra, in the spectral region located between 180 nm and 240 nm arising from the coupling of the electric dipole transition moments located on their peptide bonds, as illustrated on Fig.1.

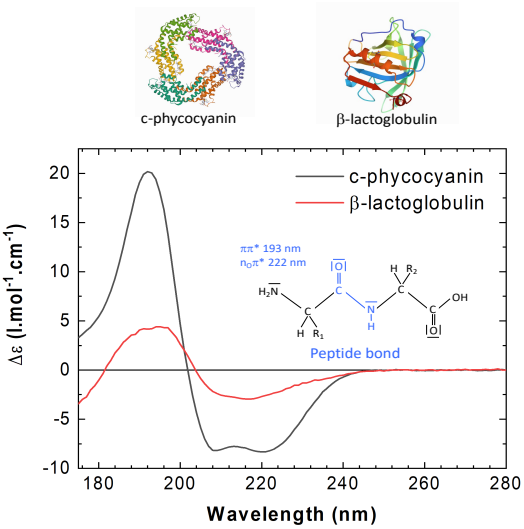

Fig. 1. CD spectra of single domain proteins: c-Phycocyanin (PDB 3O18) for α-helices and β-lactoglobulin (PDB 51O5) for β-sheets, from PCDDB IDs CD0000012000 and CD0000011000 [21]. Schematic representation of a peptide bond is given in the figure insert.

In oligonucleotides, CD signals in the spectral region below 200 nm pertain from electronic transitions located on their sugars, while in the spectral region above 220 nm, they arise from the coupling of electric dipole transition moments located on the nucleic bases and are generally used for the characterization of DNA secondary structures. Fig.2 illustrates the CD spectra of the three typical topologies of G-quadruplex structures consisting of guanine tetrad stacks formed from guanine-rich sequences.

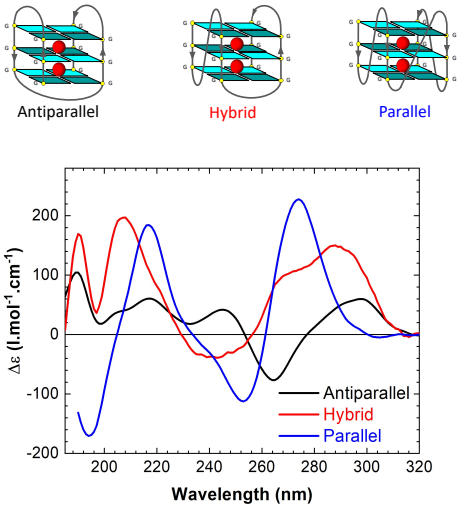

Fig. 2. CD spectra of the three typical G-quadruplex topologies: antiparallel, hybrid and parallel. CD spectra were recorded at Soleil synchrotron (DISCO line), at 25°C, for the three oligonucleotide sequences: d[5′-AGGG(TTAGGG)3-3′]/150 mM Na^+, d[5’-TTGGG(TTAGGG)3A-3’]/150 mM K^+ and d[5’-TGAGGGTGGGTAGGGTGGGTAA-3’]/150 mM K^+. Δε is given per strands of DNA.

3. Circular dichroism or ellipticity measurements?

CD and ORD, which correspond to the imaginary and real part of the complex refractive index of chiral samples, respectively, are correlated by the Kramers-Kronig transform. Although both give similar information, CD spectroscopy, which is correlated to the sample absorption, has become a much more popular method for the structural characterization of chiral samples in condensed phase. In particular, CD provides a convenient probe for monitoring the secondary structure of biomolecules in solution, under near physiological conditions. Thus CD is commonly used as complement to other biophysical methods to assess protein and DNA conformations or to monitor their structural changes upon interaction with ligands or as function of pH or temperature [15]. These measurements are usually performed with commercial CD spectrometers. Synchrotron radiations can be also used for measuring the CD spectra (SRCD) of biomolecules with the advantage of their higher flux of radiations in the far UV, enabling measurements with a better signal-to-noise (S/N) ratio [22].

In practice, CD can be measured in two different ways. The first one consists of the direct measurement of the sample differential absorbance of left- and right-circularly polarized light. In this regard, a photo-elastic modulator (PEM) for rapid polarization modulation (ca. 50 kHz) in combination with a phase-locked detection is used in most commercial spectrophotometers [23]. The second method consists of measuring the ellipticity induced by a chiral sample on a linearly polarized light beam. Principle of ellipticity measurements relies on the fact that linearly polarized light can be considered as the superposition of two equal circularly polarized waves. Ellipticity pertains from the difference in the absorption of these two waves, as schematized on Fig.3. This results in an elliptically polarized outcoming wave, the ellipticity (θ) of which is defined as the tangent of the ratio of the minor to major axis of the ellipse.

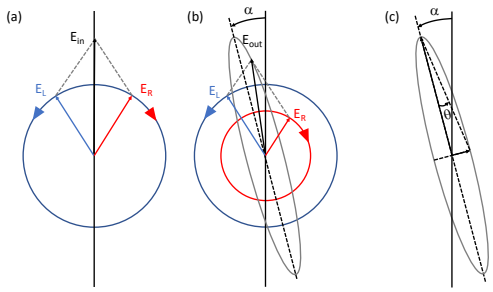

Fig. 3. (a) Decomposition of linearly polarized incoming wave into two circularly-polarized waves; (b) elliptically polarized outcoming wave stemming from the different absorption of left- and right-circularly polarized waves by a chiral medium; (c) degree of ellipticity (θ) of the outcoming wave.

Measurements of ellipticity was used in the earliest CD spectrophotometers. These measurements can be performed by placing the chiral sample between two crossed polarizers (P1 and P2). A birefringent plate (Q), such as a quarter-waveplate for instance, is added between the sample and the analyzer (P2), as shown on Fig.4. The rotation of the analyzer as function of the angle ϕ gives access to the ellipticity induced by the chiral sample on the incident linearly polarized wave.

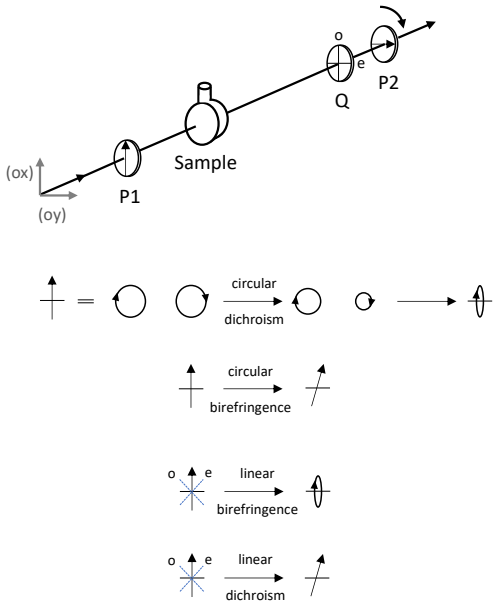

Fig. 4. Principle of conventional ellipticity measurements and effects of circular dichroism (CD), circular birefringence (ORD), linear birefringence (LB) and linear dichroism (LD) on linearly polarized light. Adapted from X. Xie, J. D. Simon, Rev. Sci. Instrum. 60, 2614 (1989) with the permission of AIP Publishing.

The effect of the different optical components on the incoming electric field can be described by the simple Jones formalism. Each optical element is described by a (2×2) matrix and the outcoming electric field reads as:

$$E^{out} = M_{analyzer} \cdot M_{\frac{\lambda}{4}} \cdot M_{sample} \cdot E^{in} \qquad (4)$$

The incoming electric field with a horizontal polarization along (ox) axis after crossing the polarizer is given by:

$$E^{in} = E_0 \begin{bmatrix} 1 \\ 0 \end{bmatrix} \qquad (5)$$

The quarter-waveplate with its fast axis oriented along (ox) and the analyzer for small angles of rotation (ϕ) are described by the Jones matrices:

$$M_{\frac{\lambda}{4}} = \begin{bmatrix} 1 & 0 \\ 0 & i \end{bmatrix} \qquad (6)$$

$$M_{analyzer} = \begin{bmatrix} 0 & \phi \\ \phi & 1 \end{bmatrix} \qquad (7)$$

The Jones matrix associated to chiral samples exhibiting small optical activity is given by [24]:

$$M_{sample} = e^{i\frac{2\pi}{\lambda}nL-\frac{\alpha L}{2}} \begin{bmatrix} 1 & \left(\frac{ORD}{2} - i\frac{CD}{4}\right) \\ \left(i\frac{CD}{4} - \frac{ORD}{2}\right) & 1 \end{bmatrix} \qquad (8)$$

The resulting output intensity reads as:

$$I_x^{out} = [E_0]^2 e^{-\alpha L}\left\{\phi^2\left[1-\left(\frac{CD}{4}\right)^2+\left(\frac{ORD}{2}\right)^2\right]-\phi\frac{CD}{2}+\left(\frac{CD}{4}\right)^2-\left(\frac{ORD}{2}\right)^2\right\} \qquad (9)$$

The output intensity has a parabolic dependence as function of ϕ, with a minimum that is proportional to the sample CD, the second orders terms being negligible:

$$\phi_{min} = \frac{\frac{CD}{4}}{\left[1-\left(\frac{CD}{4}\right)^2+\left(\frac{ORD}{2}\right)^2\right]} \sim \frac{CD}{4} \qquad (10)$$

Note that by simply removing the quarter-waveplate, the minimum output intensity becomes equal to ORD/2 giving directly access to the dispersive effect of the chiral sample on the incoming light. Both ellipticity and ORD reflect the induced ellipticity by chiral samples on the linearly polarized incoming light. They are generally expressed in millidegrees (mdeg). Ellipticity and CD can be correlated, as follow:

$$\theta\ (mdeg) = 32.982 \cdot CD \qquad (11)$$

with CD expressed in differential optical density (ΔOD).

The main drawback of direct CD measurements stems from the detection of small variations of the absorbance against a strong achiral background absorption (*i.e.* typically $\Delta\varepsilon/\varepsilon \sim 10^{-6}$-$10^{-4}$), which decreases the S/N ratio of such detection. In contrast, ellipticity measurements, which are background-free, provide an enhanced detection of the small CD variations, but with, in counterpart, an increased sensitivity to linear dichroism (LD) and linear birefringence (LB) due to the crossed-polarization detection (see Fig.4) [16,25]. As long as steady-state measurements are concerned, samples in solution are mainly isotropic and devoid of LB and LD. The strain birefringence (*i.e.* LB) in the sample cells may however cause significant offsets in the measured signals. Therefore, accurate measurements often require the use of weakly birefringent cells with minimal stress on their windows [16]. It is worth pointing that TRCD faces the same artifacts as steady-state measurements but, photoexcitation leads to additional artifacts [16,24], that are mainly due to the use of linearly polarized laser excitation. It creates an anisotropic distribution of excited molecules leading to strong LD (absorptive effect) and LB (dispersive effect) in the samples at short time scales, before the rotational diffusion of the photoexcited molecules. This lead to spurious signals in the TRCD detection, if photo-selection is not properly corrected [26,27]. We will come back on this specific point, in the next section.

4. State of art of ultrafast TRCD

4.1 Main challenges in the development of TRCD

Despite remarkable advances in femtosecond laser technology and the development of ultra-fast nonlinear spectroscopy, femtosecond TRCD spectroscopy is still very poorly developed. Because of its versatility, TRCD spectroscopy has however emerged, as early as the 1970s, combining the standard modulated CD detection of spectrophotometers with stopped-flow [28], flash photolysis [29], or temperature-jump [30] triggering methods to study the conformational changes of proteins and DNA. The temporal resolution of TRCD has been limited, for a long time, by the PEM frequency, typically 1 ms. TRCD measurements with a time resolution of a few nanoseconds could only be realized in the 1980s by Kliger et *al*., with the development of nanosecond ellipsometry [31]. The principle of their detection is illustrated in Fig.5. It is based on the measurement of the pump-induced

change in the polarization state of a highly eccentric elliptically-polarized probe transmitted by a chiral sample, with a cross-polarization geometry.

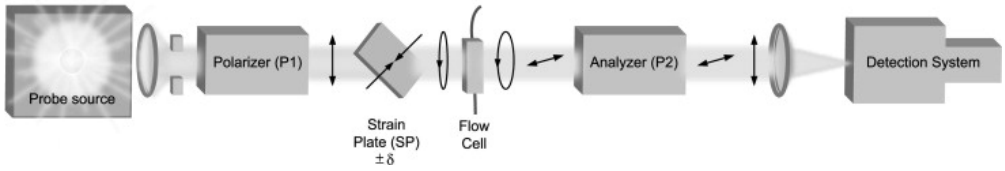

Fig. 5. Principle of nanosecond ellipsometry developed by Kliger et al. A strain plate is used to introduce a small phase delay (δ) on the linearly-polarized probe beam, to generate a highly eccentric left- or right-elliptical polarization. The change in the probe ellipticity induced by the chiral sample absorption is then monitored for retardance of the strain plate of ±δ. Reproduced from E. Chen, R. A. Goldbeck, D. S. Kliger, Methods 52, 3 (2010) with the permission of Elsevier.

As for steady-state ellipsometry, the polarization state of the probe is monitored with a combination of crossed polarizers (P1, P2) and a strained birefringent plate with a small retardation, ±δ, located before the sample. The sequential measurement of the transmitted probe by a chiral sample after photoexcitation, for strain plate retardances of ±δ, gives access to the TRCD changes:

$$S = \frac{(I_{+\delta} - I_{-\delta})}{(I_{+\delta} + I_{-\delta})} = 2.3\ \frac{CD}{\delta} \qquad (12)$$

It is worth noting that the use of a small retardation leads to the amplification of the measured TRCD signals (Eq.12). Nano-millisecond TRCD has found numerous applications for studying the conformational dynamics of biomolecules (for reviews see [15,32]). To date, the vast majority of sub-millisecond TRCD studies have been performed by Kliger et *al*. on different families of proteins [33-37]. Recently, our team has developed a nanosecond TRCD detection coupled with temperature-jump to probe the folding dynamics of some peptides and peculiar DNA structures, over a time window ranging from microseconds to seconds [38-40].

In order to reach shorter time scales, TRCD detection has to be implemented on a pump-probe set-up. This was first achieved, in the late 1980s, by Simon et *al*., who introduced a modulated TRCD detection by using a Pockels cell, on a picosecond pump-probe set-up [26]. Development of femtosecond TRCD only started more than one decade later, with the development of commercial femtosecond amplified Titanium: sapphire laser sources. In the meantime, considerable efforts have been devoted by Helbing and Cho's groups for the development of femtosecond vibrational CD (VCD) spectroscopy (for reviews, see [25,41]). Time-resolved VCD spectroscopy remains however a great challenge due to the extremely weak signals of the vibrational optical activity compared to the electronic optical activity. In fact, only very few femtosecond TRCD set-ups have been implemented so far [18,42-47]. In the following section, we discuss in details performances of these set-ups which uses similar principles of detection than steady-state CD spectroscopy.

4.2 Femtosecond TRCD

4.2.1 Direct TRCD measurements

Initially designed for single-wavelength detection [26,44,48], femtosecond TRCD has quickly evolved to broadband spectral detection, with the use of polarization-controlled white light continuum (WLC) probe initiated by Trifonov et *al*. in 2010 [43]. Modulation of the circular polarization of the probe is achieved with the combination of a quarter-waveplate and a Pockels cell located upstream of the WLC generation. Very good quality of the circular polarization over the whole broadband spectrum of the probe (*i.e*. an ellipticity lower than about 4%) could be indeed obtained under these conditions. However, the slow readout of dispersive detection using a CCD camera, at that time, required the acquisition of trains of 40 consecutive probe pulses alternating between left and right circular polarization, in order to extract the TRCD signals, which limited their accuracy to ca. 1 mOD [43]. More recently, Scholz et *al*. has implemented a similar TRCD detection employing faster readout Si photodiode arrays and reached a measurement accuracy of 0.3 mOD [47]. Despite these progresses, broadband WLC TRCD detection remains exclusively used to monitor molecular architectures exhibiting extremely large TRCD signals (>50 mdeg) in the visible spectral range, such as illustrated in Fig.6 [43,47,49,50].

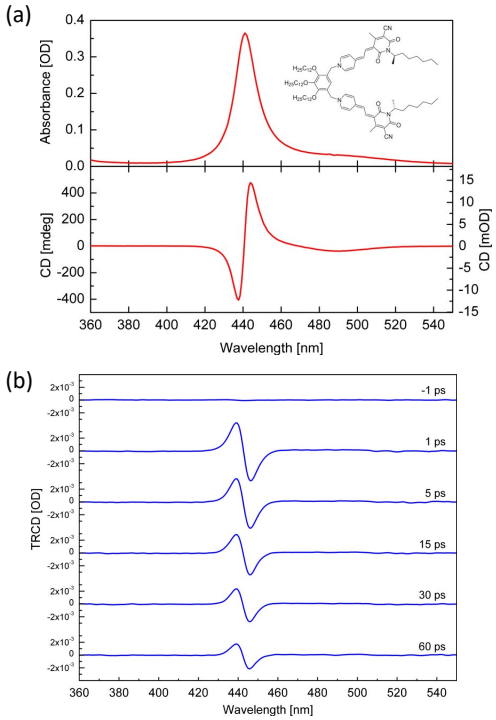

Fig.6. (a) Steady-state absorption and CD spectra of merocyanine helical nanorods dissolved in tetrahydrofuran/methylcyclohexane solution; (b) Associated TRCD spectra measured for different pump-probe delays, after excitation at 450 nm with 250 fs duration pulses. Reproduced from Trifonov A., Buchvarov I., Lorh A., Würthner F., Fiebig T. Rev. Sci. Instrum. 81, 043104 (2010) with the permission of AIP Publishing.

A significant improvement in the accuracy of broadband TRCD detection could be achieved very recently by Oppermann et *al*., by using more stable and intense broadband UV probe covering the spectral region between 370 nm and 250 nm, generated from non-collinear parametric amplification [18]. Shot-to-shot modulation of the probe polarization and detection is achieved using 50 kHz PEM coupled to fast reading-out dispersive detection with a dual-array CMOS detector, thus achieving an unprecedented accuracy of ca. 10 µDO (<1 mdeg). However, the difference between the polarization modulation frequency and the laser repetition rate (20 kHz) requires complex electronics to extract the TRCD signals from six consecutive probe pulses, as shown in Fig.7.

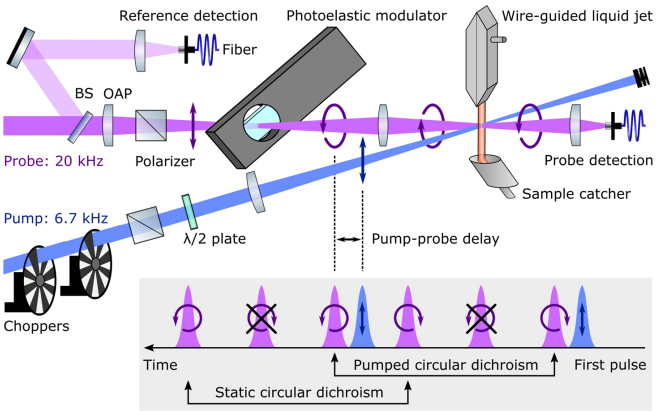

Fig.7. Broadband TRCD set-up developed by Oppermann et *al*. The probe modulation is achieved with a 50kHz PEM. The inset illustrates the sequence of six consecutive probe pulses to obtain the TRCD spectra. Reproduced with permission from Oppermann M., Bauer B., Rossi T., Zinna F., Helbing J., Lacour J., Chergui M. Optica 6, 56 (2019), DOI : 10.1364/OPTICA.6.000056 © The Optical Society.

This important advance in broadband TRCD detection enabled measurement of rapid structural changes in thioamide-substituted peptides [51]. The substitution of the peptide bonds results in a massive red shift (>60 nm) of their ππ* and nπ* transitions, allowing their detection in the 250-370 nm spectral region accessible to the broadband detection. Note that the generation of sufficiently intense and stable broad UV probes in the spectral region below 250 nm still remains a challenge to directly access the backbone dynamics of unmodified polypeptides and proteins.

4.2.2. Femtosecond ellipsometry

In contrast to direct TRCD measurements, femtosecond ellipsometry has a main of advantage of providing background-free detection with an inherent increased sensitivity. This detection geometry does not necessitate a probe modulation coupled to sophisticated synchronization electronics to extract the TRCD signals. Moreover, time-resolved ellipsometry uses linearly polarized pump and probe that is much easier to handle than circularly polarized beams, allowing easier implementation on conventional pump-probe setups. In this context, our team has developed femtosecond ellipsometry since 2006 [42]. Pump-induced changes in the probe ellipticity are measured with a cross-polarization geometry in combination with a Babinet-Soleil compensator to introduce a variable phase delay on the transmitted probe beam, as illustrated in Fig.8.

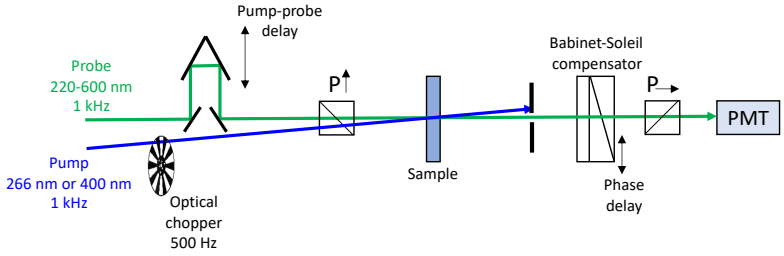

Fig.8. Single-wavelength femtosecond ellipsometric TRCD detection with a Babinet-Soleil compensator developed by Hache et coll.[42] P : polarizer; PMT: photomultiplier.

Measurements are performed in a sequential manner. For each pump-probe delay, the probe phase delay is varied of a few degrees. The resulting output intensity has a parabolic behavior (Eq. 9), which is horizontally shifted from zero retardation, for chiral samples. Alternating measurements with and without the pump with a mechanical chopper yield two parabolas as shown in Fig.9. The difference of their minima gives the pump-induced variation in the CD signals, while that of their curvature yields the differential absorbance. In contrast to broadband detection, these ellipsometric measurements readily reach a precision of 10 µOD without the need of the use of a referencing probe to correct the laser fluctuations.

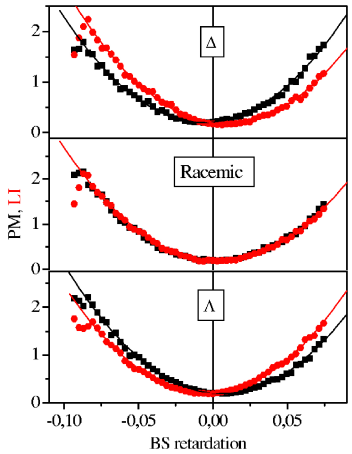

Fig.9. Variation of half of sum of the measured transmitted intensities with and with the pump (PM), their difference (LI) in arbitrary units as a function of the Babinet-Soleil retardation (in radians), for the G and D enantiomers of $[Ru(phen)_3]\cdot 2PF_6$ complexes in acetonitrile and their racemic mixture. The sign of the LI curves has been changed for easier comparison. Reproduced with permission from Hache F., Niezborala C., J. Opt. Soc. Am. 23, 2418 (2006), DOI: 10.1364/JOSAB.23.002418 © The Optical Society.

In combination with high-intensity tunable UV probe sources generated from optical parametric amplification, femtosecond ellipticity in single-wavelength detection mode has proven to be well adapted for accessing the small TRCD changes in proteins and various chiral compounds [52-57]. Fig.10 illustrates the TRCD variations measured in the R52Q mutant of Photoactive Yellow Protein, after photoexcitation at 420 nm. The fast CD change has been attributed to the fast flipping motion of the chromophore carbonyl group induced by the chromophore photoisomerization in less than 1 ps [56].

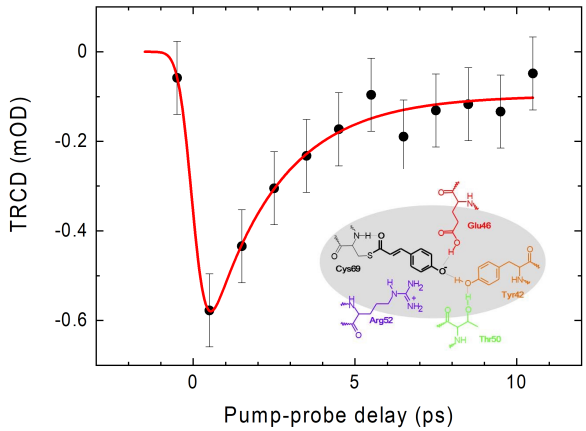

Fig.10. TRCD change in R52Q mutant measured at 332 nm, after excitation at 420 nm. The solid red line is the fit with an exponential function and a step function, convoluted with a Gaussian function (fwhm = 0.8 ps) corresponding to the instrumental response function. Insert: schematic representation of the wild type PYP active site. Adapted with permission from L. Mendonça, F. Hache, P. Changenet-Barret, P. Plaza, H. Chosrowjan, S. Taniguchi, Y. Imamoto, J. Am. Chem. Soc. 135, 14637 (2013). Copyright 2013 American Chemical Society.

Proof of principle of broadband femtosecond ellipsometric detection in the visible spectral domain was achieved by Dorkenoo et *al.* in 2010, using a broadband quarter-waveplate [45]. However, the use of such detection for comprehensive studies of the reactivity of chiral systems has not been realized. Finally, it is worth noting another advantage of cross-polarization ellipticity setups, namely their ability to perform time-resolved ORD measurements, which are accessible by analyzer rotation [42,45].

4.2.3. Pump-induced artifacts

Despite the recent developments in polarization control of ultrashort pulses and improvement in laser technologies providing increasingly stable sources, TRCD remains very sensitive to pump-induced artifacts that must be overcome for accurate measurements. As pointed out earlier, one of the main artifacts stems from the linear polarization of the pump that induces a partial orientation of the excited molecules in condensed phase namely, pump-induced LB. This artifact can be easily overcome in classical achiral transient absorption configurations using linearly polarized pump and probe beams by using the well-known "magic angle" conditions, which consist in orienting the pump and probe polarizations with an angle of 54.7° [58]. For TRCD configurations, correction of pump-induced LB depends on the probe polarization relative to the pump polarization (linear *vs*. circular). In any cases, the most straightforward way to avoid pump-induced LB would be to use randomly polarized pump pulses. This was done by Trifonov et *al*. by using a Lyot depolarizer for the measurements of strong CD variations [43]. Generation of randomly polarized excitation pulses from a linearly polarized laser beam is however tricky since it is difficult to characterize. Therefore, an alternative method introduced by Cho et *al*. for 2D spectroscopy [58,59], is generally preferred, which consists of setting an angle of 35.3° between the propagation directions of the pump and probe beams to get to the “magic angle” conditions between linearly polarized pump and circularly polarized probe [18,47].

Seminal time-resolved ellipticity experiments of Kliger et *al*. have shown that the residual polarization left by depolarizers is incompatible with cross-polarization detection, which is particularly sensitive to pump-induced LB [16,25]. Using the Jones formalism, it can be shown that pump-induced LB can be eliminated by aligning the linear polarization of the pump and probe [16,24]. Indeed, we have shown that such an alignment is particularly efficient by using a common polarizer on the pump and probe beams for the measurements of small CD variations in femtosecond ellipsometry with a Soleil-Babinet compensator [56,57]. It is worth pointing that imperfect correction of pump-induced LB can lead dominant signals in the TRCD detection and additional pernicious effects if it is combined with other artifacts, such as external birefringence (LB) in optics [16,24,46]. To limit such artifacts, it is necessary to use polarizers with high extinction coefficients (ca. 10^5) and avoid the presence of optics in between the cross-polarization detection.

5. Current developments: ultrafast single-shot ellipsometry

Ultrafast TRCD that measure the probe intensity changes have now gained enough maturity to allow the comprehensive studies of various chiral compounds in solution, at short time scales [18,43,44,49], with a major contribution from our team [19,54-57]. Both direct TRCD and ellipticity measurements requires so far, for each pump-probe delay, to introduce either a modulation of the circularly polarized probe or a variable phase delay on the linearly polarized probe. These sequential acquisition procedures are time-consuming and sensitive to pump and probe fluctuations, which decrease their S/N ratio. Hence other detection methods have been sought to

overcome this main drawback, in particular, single-shot ellipticity measurements by using heterodyne spectral interferometry or a balanced detection of the amplitude changes of the probe electric field.

5.1. Heterodyne spectral interferometric detection

Heterodyne spectral interferometric detection of the phase and amplitude changes of the probe electric field transmitted by a chiral sample has been introduced by Cho et *al.* for characterizing the optical activity in the near and mid-IR spectral region.[60] It consists of a cross-polarization detection. The transmitted chiral probe field from the sample, namely the optical activity free induction decay (OA FID) field, is mixed with a local oscillator (LO) field at a fixed delay to produce spectral interferences, as schematized in Fig.11.

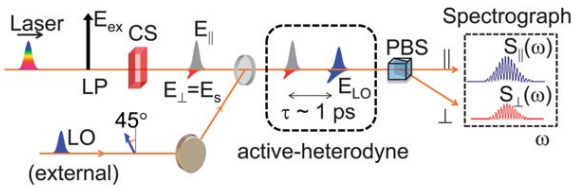

Fig.11. Heterodyne OA FID measurement scheme. LP: linear polarization; CS: chiral sample; PBS: polarizing beam splitter. Reproduced from H. Rhee, J. S. Choi, D. J. Starling, J. C. Howelld, M. Cho, Chem. Sci., 4, 4107 (2013) with permission from the Royal Society of Chemistry.

The coupling of heterodyne detection with a broadband probe allows to access to the entire CD and ORD spectra. From Fourier transform spectral interferometry (FTSI) [61], the two spectra can be recovered from the measured-parallel and perpendicular spectral interferograms ($S_{\parallel}$ and $S_{\perp}$) associated with the achiral and chiral (OA FID) components of the transmitted electric field, respectively :

$$\frac{FTSI[S_{\perp}(\omega)]}{FTSI[S_{\parallel}(\omega)]} = \frac{E_{\perp}(\omega)}{E_{\parallel}(\omega)} \propto -\frac{ORD}{2} + i\frac{CD}{4} \qquad (13)$$

First development with an analyzer required the sequential measurements of the two electric field components for perpendicular and parallel orientation with respect to the LO field. Combination with a balanced detection by using a polarizing beam splitter (Fig.11) allows to measure simultaneously both component from a single laser shot. Experimental feasibility of steady-state CD and ORD measurements in the near and mid-IR frequency range has been successfully carried out by Cho et *al*.[46,60] Active heterodyne detection was then extended to the visible spectral range by Hiramatsu et *al*., who additionally provided proof-of-principle of TRCD measurements for the ruthenium complexes, $Ru(bpy)_3Br$, in aqueous solutions [46]. However, their measurements were dominated by the contributions of pump-induced LD and LB artifacts. Singular value decomposition was required to distinguish the TRCD signals from these artifacts, which in this specific case exhibit a very distinct kinetic behavior.

In addition to polarization artifacts, the main drawback of heterodyne detection in the UV-visible frequency range is the precise control of the path length between the two arms of the interferometer, which is critical to achieve a good phase stability of typically λ/100 (*i.e.* of a few nm) [62]. Recently, a common path interferometer has been used, for a better control of the path length for active heterodyne TRCD detection in the visible and near-IR spectral domain. This allowed very fast and robust measurements of static CD and ORD spectra by using time-domain interferometry but it has not yet found application for TRCD measurements [20,63].

5.2 Single-shot balanced ellipsometry detection

In order to circumvent the phase stability problem of heterodyne detection, self-heterodyne detection coupled to a balanced detection has been developed by Cho et *al*. [60,64]. At this point, it is worth mentioning that self-heterodyne detection coupled with probe modulation and synchronous detection [65] has been adapted in a configuration suitable for femtosecond spectroscopy by Steinbacher et *al.* [66]. In the self-heterodyne geometry, the incident probe is used as the LO field, locking the phase between the OA FID and LO fields. This allows the simultaneous measurement of the amplitude of the two components of the transmitted electric field in the UV-visible spectral range, as illustrated on Fig.12. CD and ORD spectra have to be measured separately by controlling the incident probe polarization to linear or elliptical. The main advantage of the method is the CD and ORD spectra can be retrieved from one single laser shot , without any modulation of the probe [60]. As shown in Fig.12 (b-c), the steady-state CD and ORD spectra of DNA–cyanine dye complex and (±)-Ni-$(tartrate)_2$ in visible spectral range could be successfully measured. However, despite proof-of-principle of such detection for static measurements, it has never been applied for time-resolved measurements.

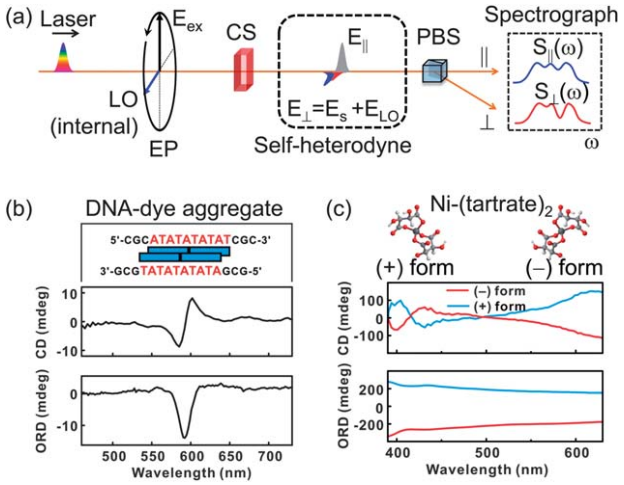

Fig.12. (a) Self-heterodyne OA FID measurement scheme, EP: elliptical polarization; LP: linear polarization; CS: chiral sample; PBS: polarizing beam splitter; (b) self-heterodyne detected CD and ORD spectra of DNA–cyanine dye complex and **(c)** (±)-Ni-(tartrate)$_2$. Reproduced from H. Rhee, J. S. Choi, D. J. Starling, J. C. Howelld, M. Cho, Chem. Sci., 4, 4107 (2013) with permission from the Royal Society of Chemistry.

Heterodyne detection implies the measurement of two signals of very different magnitudes (*ca.* 2 orders of magnitude) corresponding to the achiral ($E_{\parallel}$) and chiral ($E_{\perp}$) components of the transmitted electric field, requiring high dynamic detector to be recorded. In the same way, we recently developed an alternative cross-polarization detection method based on the measurement of the difference of two signals of nearly equal intensity, in a fully symmetric balanced detection geometry to avoid artifacts. Similarly to self-heterodyne detection, this new setup takes advantage that the transmission of linearly polarized light by a chiral sample is elliptical. The pump-induced change in the vertical and horizontal components of the elliptical polarization is measured, in this case, with the combination of a quarter-waveplate and a Wollaston prism, as illustrated on Fig.13.

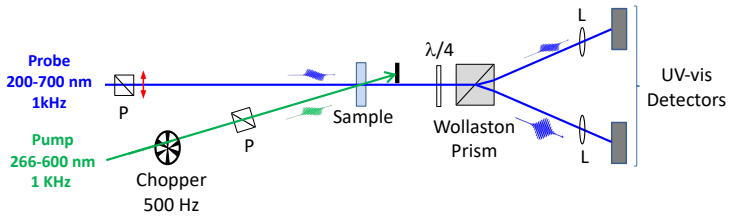

Fig.13. Balanced detection configuration for ellipsometry TRCD measurements. P : Glan Thompson polarizer. L : Lens.

The effect of the different optical components on the incident probe laser electric field can be described by Eq. 4. The analyzer being replaced by the Wollaston prism that separates the output field in two orthogonal components along (ox) and (oy) axis, respectively. For these measurements, the quarter-waveplate is oriented at +45° (clockwise) with respect to its neutral (ox) line, under these conditions the output field is expressed as:

$$E^{out}=\frac{1}{\sqrt{2}}E_0\,e^{i\frac{2\pi}{\lambda}nL-\frac{\alpha L}{2}}\begin{bmatrix}1+\dfrac{CD}{4}+i\dfrac{ORD}{2}\\ i\left(1-\left(\dfrac{CD}{4}+i\dfrac{ORD}{2}\right)\right)\end{bmatrix} \qquad (14)$$

The two intensities associated to the two orthogonal components of the output field are measured with two photodiodes or photomultipliers:

$$I_x^{out}=\left|E_x^{out}\right|^2=\frac{1}{2}E_0\,e^{-\alpha L}\left(1+\frac{CD}{2}+\frac{CD^2}{16}-\frac{ORD^2}{4}\right) \qquad (15)$$

$$I_y^{out} = \left|E_x^{out}\right|^2 = \frac{1}{2} E_0 e^{-\alpha L}\left(1 - \frac{CD}{2} + \frac{CD^2}{16} - \frac{ORD^2}{4}\right) \qquad (16)$$

The differential signal recorded by the two detectors directly yields to the sample CD, the second order terms of the denominator being negligible:

$$S_0 = 2\cdot\frac{\left(I_x^{out} - I_y^{out}\right)}{\left(I_x^{out} + I_y^{out}\right)} = CD \qquad (17)$$

With a pump-probe configuration, the differential signals measured alternatively with and without the pump yield directly to the pump-induced CD change in chiral samples:

$$S = S_{pump} - S_0 = \Delta CD \qquad (18)$$

With this balanced detection geometry, the laser probe fluctuations can be substantially compensated. However, Eq.18 is only valid for samples devoid of LB and LD artifacts. But as pointed previously, the cross-polarization geometry is very sensitive to pump-induced LB artifacts [16,25,42]. *In situ* alignment of the pump and probe linear polarization, *i.e.* with an accuracy of 0.1 degrees, is found to efficiently eliminate the pump-induced artifacts for TRCD measurements performed in standard quartz spectroscopic cells. This is illustrated in Fig.14, for measurements performed on the two enantiomers (Λ and Δ) of $[Ru(phen)_3]\cdot 2PF_6$ complexes in acetonitrile and their racemic mixture around 270 nm.

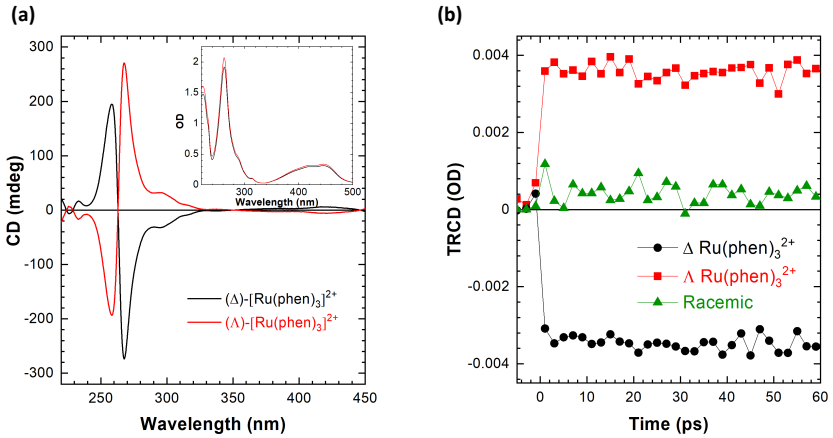

Fig.14. (a) Steady-state absorption (inset) and CD spectra and (b) single-shot TRCD measurements performed for the Δ and Λ enantiomers of $[Ru(phen)_3]\cdot 2PF_6$ and their racemic mixture in acetonitrile around 270 nm, after excitation at 400 nm. Signals were averaged over 50 laser shots.

Due to the propeller-twist arrangement of their phenanthroline ligands, these complexes display strong CD signals in the spectral region between 230 nm and 330 nm shown in Fig.13 (a). Upon excitation of the lowest singlet excited state of $[Ru(phen)_3]^{2+}$ pertaining from a metal-to-ligand charge transfer (^{1}MLCT) state, these complexes undergo a fast intersystem crossing in the sub-100-fs regime, leading to the formation of a long-lived triplet state (^{3}MLCT, $\tau \approx 0.6$ µs) with a quantum yield close to the unity. The UV-visible excitation reduces the excitonic coupling between the ligands, producing TRCD changes as shown on Fig.13 (b) [67]. The balanced detection allowed us to measure the TRCD signals of $[Ru(phen)_3]^{2+}$ with very short acquisition times (*i.e.* 50 laser shots) with an accuracy of 0.1 mOD. An accuracy of 30 µOD can be typically reached for longer acquisitions over 300 laser shots. This corresponds to a diminution of the acquisition times by a factor of ca. 20 in comparison with our TRCD setup using a Babinet-Soleil compensator. Our first single-shot TRCD measurements with this cross-polarization geometry are thus very promising. It is also worth pointing that all of these measurements were performed in standard spectroscopic quartz cells that could explain the observation of the small pump-induced residual artifact around the time zero, in the racemic. Importantly, those artifacts can be readily identified and minimized with measurements performed as function of the pump polarization. To overcome these residual signals in future experiments that may become troublesome for measurements of low TRCD signals in biomolecules, the use of low birefringent sample cells is currently under study.

5. Conclusion and perspectives

TRCD pump-probe spectroscopy has the potential to directly interrogate the conformational change of biomolecules by combining both high temporal resolution with structural sensitivity that is not accessible to conventional transient absorption spectroscopy. But despite this great potential, the implementation of TRCD spectroscopy on femtosecond pump-probe setups has remained very scarce for long, due to the fundamental limitations encountered in the detection of small signal variations (*i.e.* 10^{-3}-10^{-5} OD) prone to pump-induced polarization artifacts. Therefore, over the past 20 years, femtosecond TRCD spectroscopy has been mostly limited to proof-of-principle and very few studies of biomolecules could be performed. With the development of the ultrafast laser technologies and their related optics and detection, broadband TRCD measurements by shot-to-shot modulation of the circular polarization of the probe have now become feasible with an accuracy of a few μOD. However, these sequential measurements require a complex synchronous detection and are quite sensitive to laser fluctuations. To overcome these difficulties, the development of ellipticity measurements provides great promise since they enable single-shot detection geometry that considerably reduces the acquisition times for precise TRCD measurements. This very simple detection scheme does not require any polarization modulation. We have been able to demonstrate for the first time the feasibility of time-resolved measurements largely free of pump-induced artifacts. While single-wavelength ellipsometric detection has been already used to probe structural changes in biomolecule backbones in the 220-300 nm spectral range, the future challenge for TRCD lies in the generation of broadband probe sufficiently intense and stable to measure entire spectra in this spectral range. With the development of high repetition rate Ytterbium laser sources, a significant increase in the S/N ratio in single-shot ellipsometric detection is expected, making TRCD measurements with a few μOD accuracy easier. Finally, although the full potential of TRCD spectroscopy is not yet known, theoretical studies have demonstrated the ability of TRCD experiments and their extension to multidimensional spectroscopy to probe the delocalization of excited states in multichromophoric assemblies and identify of the origin of their coherences [68-70]. So far, only one two-dimensional chiral spectroscopy experiment has been performed to characterize the complex relaxation dynamics of light harvesting 2 complexes of Rhodobacter sphaeroides in the visible-near IR spectral region [71].

---

[a] e-mail: pascale.changenet-barret@polytechnique.edu

The authors thank F. Wien from DISCO beamline at Synchrotron Soleil for his assistance for the SRCD measurement of G-quadruplexes (proposals 20170318 and 20201655).

References (10 points)

[1] M. Maiuri, M. Garavelli, and G. Cerullo, J. Am. Chem. Soc. **142** (1), 3 (2020).
[2] C. Fang and L. Tang, Annu. Rev. Phys. Chem. **71**, 239 (2020).
[3] J. Cao, R. J. Cogdell, D. F. Coker, H.-G. Duan, J. Hauer, U. Kleinekathöfer, T. L. C. Jansen, T. Mančal, R. J. D. Miller, J. P. Ogilvie, V. I. Prokhorenko, T. Renger, H.-S. Tan, R. Tempelaar, M. Thorwart, E. Thyrhaug, S. Westenhoff, and D. Zigmantas, Sci. Adv. **6**, eaaz4888 (2020).
[4] S. Biswas, J. W. Kim, X. Zhang, and G. D. Scholes, Chem. Rev. **122** (3), 4257 (2022).
[5] J. Bredenbeck, J. Helbing, C. Kolano, and P. Hamm, ChemPhysChem **8**, 1747 (2007).
[6] N. T. Hunt, Chem. Soc. Rev. **38**, 1837 (2009).
[7] P. Hamm and M. Zanni, *Concepts and Methods of 2D Infrared Spectroscopy*. (Cambridge University Press, Cambridge, 2011).
[8] M. K. Petti, J. P. Lomont, M. Maj, and M. T. Zanni, J. Phys. Chem. B **122**, 1771 (2018).
[9] H. Kim and M. Cho, Chem. Rev. **113**, 5817 (2013).
[10] P. Kukura, D. W. McCamant, and R. A. Mathies, Annu. Rev. Phys. Chem. **58**, 461 (2007).
[11] D. Buhrke and P. Hildebrandt, Chem. Rev. **120** (7), 3577 (2020).
[12] H. Kuramochi and T. Tahara, J. Am. Chem. Soc. **143** (26), 9699 (2021).
[13] G. Branden and R. Neutze, Science **373**, eaba0954 (2021).
[14] N. Berova, K. Nakanishi, and R. W. Woody, *Circular Dichroism. Principles and Applications.*, Second Edition ed. (2000).
[15] G. D. Fasman, *Circular Dichroism and the Conformational Analysis of Biomolecules*. (Springer New York, NY, 2010).
[16] S. C. Björling, R. A. Goldbeck, S. J. Milder, C. E. Randall, J. W. Lewis, and D. S. Kliger, J. Phys. Chem. **95** (12), 4685 (1991).
[17] A. Steinbacher, H. Hildenbrand, S. Schott, J. Buback, M. Schmid, P. Nuernberger, and T. Brixner, Opt. Express **25**, 21735 (2017).
[18] M. Oppermann, B. Bauer, T. Rossi, F. Zinna, J. Helbing, J. Lacour, and M. Chergui, Optica **6**, 56 (2019).
[19] F. Hache and P. Changenet, Chirality **33**, 747 (2021).
[20] S. Ghosh, G. Herink, A. Perri, F. Preda, C. Manzoni, D. Polli, and G. Cerullo, ACS Photonics **8**, 2234 (2021).
[21] L. Whitmore, B. Woollett, A. J. Miles, D. P. Klose, R. W. Janes, and B. A. Wallace, Nucleic Acids Res. **39**, D480 (2011).
[22] J. G. Lees and B. A. Wallace, Spectroscopy **16**, 121 (2002).
[23] A. F. Drake, J. Phys. E: Sci. Instrum. **19**, 170 (1986).
[24] X. Xie and J. D. Simon, J. Opt. Soc. Am. B **7** (8), 1673 (1990).
[25] B. Dutta and J. Helbing, Opt. Express **23**, 16449 (2015).
[26] X. Xie and J. D. Simon, Rev. Sci. Inst. **60**, 2614 (1989).
[27] C. M. Einterz, J. W. Lewis, S. J. Milder, and D. S. Kliger, J. Phys. Chem. **89** (18), 3845 (1985).
[28] P. M. Bayley, Prog. Biophys. Molec. Biol. **37** (3), 149 (1981).
[29] F. A. Ferrone, J. J. Hopfield, and S. E. Schnatterly, Rev. Sci. Inst. **45**, 1392 (1974).
[30] M. Anson, S. R. Martin, and P. M. Bayley, Rev. Sci. Inst. **48**, 953 (1977).
[31] D. S. Kliger and J. W. Lewis, Rev. Chem. Intermed. **8** (4), 367 (1987).
[32] E. Chen, R. A. Goldbeck, and D. S. Kliger, Methods **52**, 3 (2010).
[33] Y. G. Thomas, I. Szundi, J. W. Lewis, and D. S. Kliger, Biochemistry **48**, 12283 (2009).
[34] J. A. Clinger, E. Chen, D. S. Kliger, and G. N. P. Jr., J. Phys. Chem. B **125**, 202 (2021).
[35] S. J. Milder, S. C. BjorlingI, I. D. Kuntz, and D. S. Kliger, Biophys. J. **53**, 659 (1988).
[36] E. Chen and D. S.Kliger, Inorganica Chimica Acta **242** (1-2), 149 (1996).
[37] S. C. Bjorling, R. A. Goldbeck, S. J. Paquette, S. J. Milder, and D. S. Kliger, Biochemistry **35**, 8619 (1996).
[38] M.-T. Khuc, L. Mendonça, S. Sharma, X. Solinas, M. Volk, and F. Hache, Rev. Sci. Inst. **82**, 054302 (2011).
[39] L. Mendonça, A. Steinbacher, R. Bouganne, and F. Hache, J. Phys. Chem. B **118**, 5350 (2014).
[40] K. Laouer, M. Schmid, F. Wien, P. Changenet, and F. Hache, J. Phys. Chem. B **125**, 8088 (2021).
[41] H. Rhee, J. S. Choi, D. J. Starling, J. C. Howelld, and M. Cho, Chem. Sci. **4**, 4107 (2013).
[42] C. Niezborala and F. Hache, J. Opt. Soc. Am. B **23**, 2418 (2006).
[43] A. Trifonov, I. Buchvarov, A. Lohr, F. Würthhner, and T. Fiebig, Rev. Sci. Instrum. **81**, 043104 (2010).
[44] J. Meyer-Ilse, D. Akimov, and B. Dietzek, J. Phys. Chem. Lett. **3**, 182 (2012).
[45] L. Mangot, G. Taupier, M. Romeo, A. Boeglin, O. Cregut, and K. D. Dorkenoo, Opt. Lett. **35**, 381 (2010).
[46] K. Hiramatsu and T. Nagata, J. Chem. Phys. **143**, 121102 (2015).
[47] M. Scholz, M. Morgenroth, M. J. Cho, D. H. Choi, K. Oum, and T. Lenzer, J Phys Chem. Lett. **10**, 5160 (2019).

[48] T. Dartigalongue and F. o. Hache, J. Chem. Phys. **123**, 184901 (2005).
[49] M. Morgenroth, M. Scholz, T. Lenzer, and K. Oum, J. Phys. Chem. C **124**, 10192 (2020).
[50] M. Morgenroth, M. Scholz, M. J. Cho, D. H. Choi, K. Oum, and T. Lenzer, Nat. Com. **13**, 210 (2022).
[51] M. Oppermann, J. Spekowius, B. Bauer, R. Pfister, M. Chergui, and J. Helbing, J. Phys. Chem. Lett. **10**, 2700 (2019).
[52] T. Dartigalongue and F. Hache, Chem. Phys. Lett. **415**, 313 (2005).
[53] T. Dartigalongue and F. Hache, Chirality **18** (4), 273 (2006).
[54] T. Dartigalongue, C. Niezborala, and F. Hache, Phys. Chem. Chem. Phys. **9**, 1611 (2007).
[55] F. Hache, M. Khuc, J. Brazard, P. Plaza, M. Martin, G. Checcucci, and F. Lenci, Chem. Phys. Lett. **483**, 133 (2009).
[56] L. Mendonca, F. Hache, P. Changenet-Barret, P. Plaza, H. Chosrowjan, S. Taniguchi, and Y. Imamoto, J. Am. Chem. Soc. **135**, 14637 (2013).
[57] M. Schmid, L. Martinez-Fernandez, D. Markovitsi, F. Santoro, F. Hache, R. Improta, and P. Changenet, J. Phys. Chem. Lett. **10**, 4089 (2019).
[58] S. Schott, A. Steinbacher, J. Buback, P. Nuernberger, and T. Brixner, J. Phys. B: At. Mol. Opt. Phys. **47**, 124014 (2014).
[59] M. Cho, J. Chem. Phys. **119** (14), 7003 (2003).
[60] I. Eom, S.-H. Ahn, H. Rhee, and M. Cho, Phys. Rev. Lett. **108**, 103901 (2012).
[61] L. Lepetit, G. Cheriaux, and M. Joffre, J. Opt. Soc. Am. B **12**, 2467 (1995).
[62] S. Biswas, J. W. Kim, X. Zhang, and G. D. Scholes, Chem. Rev. **122**, 4257 (2022).
[63] F. Preda, A. Perri, J. Réhaut, B. Dutta, J. Helbing, G. Cerullo, and D. Polli, Opt. Lett. **43** (8), 1882 (2018).
[64] I. Eom, S.-H. Ahn, H. Rhee, and M. Cho, Opt. Express **19** (10), 10017 (2011).
[65] J.-Y. Lee and D.-C. Su, Opt. Comm. **256**, 337 (2005).
[66] A. Steinbacher, J. Buback, P. Nuernberger, and T. Brixner, Opt. Express **20** (11), 11838 (2012).
[67] C. Niezborala and F. Hache, J. Phys. Chem. A **111** (32), 7732 (2007).
[68] D. I. H. Holdaway, E. Collini, and A. Olaya-Castro, J. Chem. Phys. **114**, 194112 (2016).
[69] D. I. H. Holdaway, E. Collini, and A. Olaya-Castro, Opt. Express **25**, 6383 (2017).
[70] N. Mann, P. Nalbach, S. Mukamel, and M. Thorwart, J. Chem. Phys. **141**, 234305 (2014).
[71] A. F. Fidler, V. P. Singh, P. D. Long, P. D. Dahlberg, and G. S. Engel, Nat. Commun. **5**, 3286 (2014).